Simulation of solar radiative transfer under different atmospheric conditions. Part I. The deterministic atmosphere

T.B. Zhuravleva

Institute of Atmospheric Optics,
Siberian Branch of the Russian Academy of Sciences, Tomsk

Received September 10, 2007

The model of solar radiative transfer under different atmospheric conditions including spatially inhomogeneous and stochastic clouds is presented. The statistical algorithms for calculation of fluxes and brightness fields in the plane-parallel deterministic model of the atmosphere are described. The results of comparison of radiation calculations in spatially inhomogeneous clouds, performed as a part of the international project "Intercomparison of 3D Radiation Codes" are given. The approaches to accounting for the molecular absorption, implemented in the model, are described, which are based on the transmission function and the photon survival probability.

Introduction

Numerical simulation of fluxes and brightness fields of the solar radiation is unavoidable stage in solution of a wide range of direct and inverse problems of the atmospheric optics. To do this, many scientific centers develop codes designed for calculation of the radiative characteristics under different atmospheric conditions. Most of them are aimed at simulation of the shortwave solar radiative transfer in the *horizontally homogeneous model* of the atmosphere[1–3]; however, in the last decade, in view of the invention of procedures for generation of actual cloud fields, the algorithms of the radiation calculations in the presence of *deterministic spatially inhomogeneous* clouds are actively developed.[1,4] The difference in the radiation codes is connected with different methods of solution of the radiative transfer equation (RTE) and methods of accounting for the molecular absorption (see the reviewing papers[1–4] and the references therein). In the framework of the *statistical approach* to the description of the radiative transfer in the cloudy atmosphere, some codes involve procedures designed for calculation of the ensemble-*average* realizations of characteristics of the cloud and radiation fields.[5,6] The features of these algorithms stem from the specificity of the *stochastic* cloud model, realized in each particular code.

For 30 years, the algorithms of the statistical simulation, designed for description of the optical radiative transfer in the Earth's atmosphere have been developed at IAO SB RAS (Tomsk). These algorithms are successfully used for solution of lidar sensing problems, vision theory, propagation of solar and thermal radiation under conditions of the stochastic clouds, etc. (see, e.g., Refs. 5, 7–10 and references therein).

In this paper, a unified description of the Monte Carlo algorithms for calculation of shortwave radiation characteristics in a *deterministic* atmosphere (horizontally homogeneous atmosphere, containing spatially inhomogeneous clouds) is presented, developed by the author or with her direct participation.

Section 1 presents basic relations, traditionally used for simulation of radiation transfer in the deterministic atmosphere by the Monte Carlo method (they are extensively described in the monographs of national and foreign specialists.[11–14]). Statistical algorithms for calculation of fluxes and brightness fields, as well as results of testing in the plane-parallel horizontally homogeneous model of the atmosphere and in the presence of the vertically and horizontally inhomogeneous clouds are described in Sections 2 and 3, respectively. Methods of accounting for the molecular absorption (on the basis of the atmospheric gas transmission function $T_{\Delta\lambda}$ and through the photon survival probability) are presented in Section 4.

1. Monte Carlo method for solution of the radiative transfer equation in a deterministic medium

The monochromatic radiation transfer in an optically isotropic medium without taking into account the polarization effects and refraction is considered under the assumption that the radiation field is stationary. In the framework of the made approximations, the RTE in theory of Monte Carlo methods is written with respect to the *particle flux density* $\Phi(\lambda, \mathbf{r}, \omega)$ at the point $\mathbf{r} = (x, y, z)$ and in the direction ω:

$$\omega\nabla\Phi(\lambda,\mathbf{r},\omega) = -\sigma(\lambda,\mathbf{r})\Phi(\mathbf{r},\omega) + \frac{\sigma_s(\mathbf{r})}{2\pi}\times$$

$$\times\int_{4\pi}\Phi(\lambda,\mathbf{r},\omega')g(\lambda,\mathbf{r},(\omega',\omega))\mathrm{d}\omega' + \Phi_0(\lambda,\mathbf{r},\omega), \quad (1)$$

0235-6880/08/02 81-15 $02.00

and with respect to the *particle collision density* $f(\lambda, \mathbf{r}, \omega) = \sigma(\lambda, \mathbf{r})\,\Phi(\lambda, \mathbf{r}, \omega)$:

$$f(\lambda,\mathbf{r},\omega) = \int\limits_{G}\int\limits_{4\pi}\sigma(\lambda,\mathbf{r})\sigma_s(\lambda,\mathbf{r}')g\big(\lambda,\mathbf{r},(\omega',\omega)\big)\times$$
$$\times\exp\{-\tau(\lambda,\mathbf{r}',\mathbf{r})\}/[2\pi|\mathbf{r}-\mathbf{r}'|^2\,\sigma(\lambda,\mathbf{r}')]\times$$
$$\times\delta\{\omega-(\mathbf{r}-\mathbf{r}')/|\mathbf{r}-\mathbf{r}'|\}f(\lambda,\mathbf{r}',\omega')\mathrm{d}\mathbf{r}'\mathrm{d}\omega' + \psi(\lambda,\mathbf{r},\omega), \quad (2)$$

where λ is the wavelength; $\Phi_0(\lambda, \mathbf{r}, \omega)$ and $\psi(\lambda, \mathbf{r}, \omega)$ are the distribution densities of the internal sources and initial collisions; $\sigma(\lambda, \mathbf{r})$ and $\sigma_s(\lambda, \mathbf{r})$ are the coefficients of radiation extinction and scattering at the point $\mathbf{r}$, respectively; $\tau(\lambda, \mathbf{r}', \mathbf{r})$ is the optical pathlength between the points $\mathbf{r}'$ and $\mathbf{r}$; $g[\lambda, \mathbf{r}, (\omega', \omega)]$ is the scattering phase function, which depends only on $\mu = \cos\theta = (\omega', \omega)$, the cosine of the angle θ between the vectors of unit length ω' and ω, and which satisfies the normalization condition

$$\int\limits_{-1}^{1} g(\lambda,\mathbf{r},\mu)\mathrm{d}\mu = 1.$$

From here on, in the consideration of the characteristics of the radiation field and optical characteristics of the medium, we will drop the parameter λ.

Integral equation (2) is represented in the operator form as:

$$f(\mathbf{x}) = \int\limits_{X} k(\mathbf{x}',\mathbf{x})f(\mathbf{x}')\mathrm{d}\mathbf{x}' + \psi(\mathbf{x}'),$$

or

$$f = Kf + \psi, \quad (3)$$

where X is the phase space of coordinates and directions $\mathbf{x} = (\mathbf{r}, \omega) \in X = R^3 \times \Omega$: $\mathbf{r} \in R^3$, $\omega \in \Omega$ (Ω is the sphere of the unit radius), and the generalized kernel is

$$k(\mathbf{x}',\mathbf{x}) = \big(\sigma_s(\mathbf{r}')g[\mathbf{r}',(\omega',\omega)]\exp\{-\tau(\mathbf{r}',\mathbf{r})\}\sigma(\mathbf{r})\big)\times$$
$$\times\delta\{\omega-(\mathbf{r}-\mathbf{r}')/|\mathbf{r}-\mathbf{r}'|\}/[2\pi\sigma(\mathbf{r}')|\mathbf{r}-\mathbf{r}'|^2]. \quad (4)$$

The considered radiation characteristics, (flux and intensity of the scattered radiation) are represented in the form of the linear functional of equation (3) solution:

$$I_h = (f,h) = \int\limits_{X} f(\mathbf{x})h(\mathbf{x})\mathrm{d}\mathbf{x} = \sum_{n=0}^{\infty}(K^n\psi,h),$$
$$\big[K^n\psi\big](\mathbf{x}) = \overbrace{\int\limits_{X}\ldots\int\limits_{X}}^{n}\psi(\mathbf{x}_0)k(\mathbf{x}_0,\mathbf{x}_1)\ldots k(\mathbf{x}_{n-1},\mathbf{x})\mathrm{d}\mathbf{x}_0\ldots\mathrm{d}\mathbf{x}_{n-1}, \quad (5)$$

where $h(\mathbf{x}) \geq 0$ depends on the calculated functional.

According to Refs. 11 and 12, the random quantity is simulated for calculation of I_h

$$\eta = \sum_{n=0}^{N_0} Q_n h(\mathbf{x}_n), \quad (6)$$

where the weights Q_n are defined by the following formulas:

$$Q_0 = \psi(\mathbf{x}_0)/r_0(\mathbf{x}_0),\ Q_n = Q_{n-1}k(\mathbf{x}_{n-1},\mathbf{x}_n)/r(\mathbf{x}_{n-1},\mathbf{x}_n). \quad (7)$$

The Markov chain is determined by the initial $r_0(\mathbf{x})$ and transitional $r(\mathbf{x}', \mathbf{x})$ collision densities, respectively, while N_0 is the random number of the state, immediately preceding to termination of the Markov chain (absorption or escape from the medium). The basic statement of the set of the local estimate methods is that the mathematical expectation of the random quantity (6) is equal to the sought linear functional

$$(f,h) = M\eta = M\sum_{n=0}^{N_0} Q_n h(\mathbf{x}_n), \quad (8)$$

provided the following conditions are satisfied

$$r_0(\mathbf{x}) \neq 0 \text{ for } \psi(\mathbf{x}) \neq 0,\ r(\mathbf{x}',\mathbf{x}) \neq 0 \text{ for } k(\mathbf{x}',\mathbf{x}) \neq 0,$$
$$\|K^{n_0}\| < 1, \text{ where } K(\mathbf{x}',\mathbf{x}) = |k(\mathbf{x}',\mathbf{x})|.$$

In a number of cases, the linear functional I_h is estimated using the method of *adjoin walks*, based on the consideration of the adjoin equation

$$f^*(\mathbf{x}) = \int\limits_{X} k(\mathbf{x}',\mathbf{x})f^*(\mathbf{x}')\mathrm{d}\mathbf{x}' + \varphi(\mathbf{x}),$$
$$f^* = K^*f^* + \varphi.$$

It follows from the optical reciprocity theorem $(f, \varphi) = (f^*, \psi)$ that

$$I_h = \int\limits_{R}\int\limits_{\Omega} f_1^*(\mathbf{r},\omega)\Phi_0(\mathbf{r},-\omega)/\sigma(\mathbf{r})\mathrm{d}\omega\mathrm{d}\mathbf{r}, \quad (9)$$

where f_1^* is the collision density, corresponding to the transfer equation with the source density $p_1(\mathbf{r}, \omega) = h(\mathbf{r}, \omega)\sigma(\mathbf{r})$.[11,15] In accordance with Eq. (9), calculation of I_h by the method of adjoin walks is reduced to estimation of the mathematical expectation of the random quantity

$$\eta = \sum_{n=0}^{N_0} Q_n\psi_1(\mathbf{x}_n),\ \psi_1(\mathbf{x}) = \Phi_0(\mathbf{r},-\omega)/\sigma(\mathbf{r}). \quad (10)$$

2. Plane-parallel horizontally homogeneous model of the atmosphere

A wide range of direct and inverse problems of the atmospheric optics, both under clear sky conditions and in the presence of clouds, is presently solved in terms of the *plane-parallel model of the Earth atmosphere*. In terms of this approximation, we introduce the Cartesian coordinate system $OXYZ$

such that the OZ axis is oriented perpendicular to the Earth surface.

Assume that the atmosphere top boundary $z = H_{\text{atm}}^{\text{top}}$ is illuminated by monochromatic flux of solar radiation in the direction $\boldsymbol{\omega}_\odot$. Such a source is described by the function

$$S(\lambda, \mathbf{r}, \boldsymbol{\omega}) = I_0(\lambda)\delta(\lambda - \lambda_0)\delta(z - H)\delta(\boldsymbol{\omega} - \boldsymbol{\omega}_\odot),$$

where $I_0(\lambda) = \pi S_\lambda$ is the spectral solar constant and $H = H_{\text{atm}}^{\text{top}}$. The direction $-\boldsymbol{\omega}_\odot$, opposite to the radiation incidence direction $\boldsymbol{\omega}_\odot$, is characterized by the solar zenith angle $\xi_\odot$ between the OZ axis and the vector $-\boldsymbol{\omega}_\odot$, as well as by the azimuth angle $\varphi_\odot$, measured counterclockwise from the positive direction of the OX axis in the XOY plane: $(-\boldsymbol{\omega}_\odot) = (\xi_\odot, \varphi_\odot)$. The directing cosines $\boldsymbol{\omega}_\odot$ are, respectively: $a_\odot = -\sin\xi_\odot\cos\varphi_\odot$, $b_\odot = -\sin\xi_\odot\sin\varphi_\odot$, and $c_\odot = -\cos\xi_\odot$. The zenith ξ and azimuth φ angles of the viewing direction $\boldsymbol{\omega} = (\xi, \varphi)$ are measured from the positive directions of the OZ and OX axes of the Cartesian coordinate system; the directing cosines of the vector $\boldsymbol{\omega} = (a, b, c)$. The illumination of the atmospheric top boundary $E_0 = I_0|c_\odot|$.

2.1. Radiative transfer equation in the horizontally homogeneous atmosphere

Under assumption of the atmosphere horizontal homogeneity, it is considered that the optical characteristics and, correspondingly, the characteristics of the radiation field depend only on one spatial coordinate z (the height above the Earth surface).

In this case, the one-dimensional ($1D$) equation (2) with respect to the collision density is written as:

$$f(z,\boldsymbol{\omega}) = \frac{\sigma(z)}{|c|}\int\limits_{E_z}\frac{\sigma_s(z')}{\sigma(z')}\left[\int\limits_{4\pi}\frac{g(z',\mu)}{2\pi}f(z',\boldsymbol{\omega}')\mathrm{d}\boldsymbol{\omega}'\right]\times$$

$$\times\exp\left(-\frac{1}{|c|}\tau(z',z)\right)\mathrm{d}z' + \sigma(z)j(z)\delta(\boldsymbol{\omega} - \boldsymbol{\omega}_\odot), \qquad (11)$$

$$E_z = \begin{cases}(0,z), & c > 0,\\ (z,H), & c < 0.\end{cases}$$

Here, the density of unscattered radiation is

$$j(z) = I_0\exp\{-\tau(z,H)/|c_\odot|\},$$

while the optical depth is

$$\tau(z_1,z_2) = \left|\int\limits_{z_1}^{z_2}\sigma(z')\mathrm{d}z'\right|. \qquad (12)$$

2.2. Optical model of the horizontally homogeneous atmosphere

It is assumed that the atmosphere consists of N_{lay} layers, within each the pressure p, the temperature T, and the concentration of the atmospheric gases are constant (Fig. 1). Each ith layer ($1 \le i \le N_{\text{lay}}$) is characterized by the height of the top H_i^{top} and bottom H_i^{bot} boundaries: $H_1^{\text{bot}} = 0$, $H_{N_{\text{lay}}}^{\text{top}} = H_{\text{atm}}^{\text{top}}$. The optical characteristics of the atmosphere within each ith layer $H_i^{\text{bot}} \le z \le H_i^{\text{top}}$ are constant.

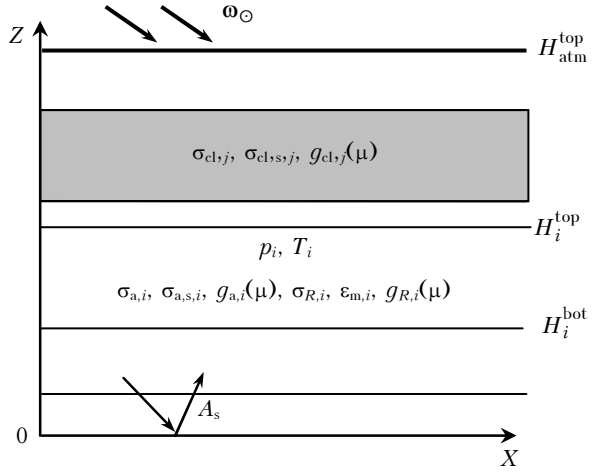

Fig. 1. Model of the plane-parallel horizontally homogeneous atmosphere of the Earth.

The optical model of the *molecular-aerosol atmosphere* is completely defined, if each ith layer is specified by the coefficients of aerosol extinction $\sigma_a(\lambda, z) = \sigma_{a,i}(\lambda)$ and scattering $\sigma_{a,s}(\lambda, z) = \sigma_{a,s,i}(\lambda)$, aerosol scattering phase function $g_a(\lambda, z, \mu) = g_{a,i}(\lambda, \mu)$, coefficients of molecular scattering $\sigma_R(\lambda, z) = \sigma_{R,I}$ and absorption $\varepsilon_m(\lambda, z) = \varepsilon_{m,I}$, as well as the Rayleigh scattering phase function $g_R(\mu) = 3(1 + \mu^2)/8$. When considering the *cloudy* atmosphere, it is assumed that the clouds are overcast and occupy the layer as a whole. Therefore, in description of the model, it is necessary to specify the cloud layer numbers ($N_{\text{cl},1}$, $N_{\text{cl},2}$, ..., $N_{\text{cl},M}$, M is the number of layers occupied by clouds) and within each of them, in addition to the molecular-aerosol characteristics, to determine the cloud particle extinction $\sigma_{\text{cl}}(\lambda, z) = \sigma_{\text{cl},N_{\text{cl},i}}(\lambda)$ and scattering $\sigma_{\text{cl,s}}(\lambda, z) = \sigma_{\text{cl,s},N_{\text{cl},i}}(\lambda)$ coefficients, as well as the scattering phase function $g_{\text{cl}}(\lambda, z, \mu) = g_{\text{cl},N_{\text{cl},i}}(\lambda, \mu)$.

The stratification and spectral behavior of the aerosol optical characteristics are specified on the basis of commonly adopted models,[16–21] while the molecular scattering coefficients — on the basis of LOWTRAN7 model.[21] The cloud optical characteristics, required for RTE solution, are calculated in the framework of the Mie theory.[22]

It is assumed that the incident radiation is reflected from the horizontally homogeneous underlying surface according to the Lambert law, which suggests that the probability of photon reflection and the direction $\boldsymbol{\omega}$ of photon travel after the reflection do not depend on the direction of the incidence on the surface.[11,13,15,23,24] The cosine of the angle between the outward normal $\mathbf{n}$ to the surface and the direction of travel of the reflected photon $\mu = \cos\theta = (\boldsymbol{\omega}, \mathbf{n})$ is the random quantity with the probability density $p(\mu) = 2\mu$, $0 \le \mu \le 1$. The azimuth angle φ is distributed uniformly in the interval $[0, 2\pi]$. In this case, the reflection coefficient is

$$\rho(\boldsymbol{\omega}, \boldsymbol{\omega}') = p(\mu)A_s/(2\pi),$$

where A_s is the surface albedo.

Note that the above-listed characteristics pertain to the monochromatic radiation. However, they can also be tailored to a finite spectral interval $\Delta\lambda = (\lambda_1, \lambda_2)$, provided the optical properties of the medium within $\Delta\lambda$ change insignificantly. In the case of the selective absorption, $\varepsilon_m(\lambda)$ may be strongly oscillating functions even within very narrow spectral intervals (such a situation takes place in the absorption bands of water vapor, carbon dioxide, and other atmospheric gases). In these cases, the gas absorption is taken into account based on the transmission function $T_{\Delta\lambda}(l)$, which is the photon survival probability on the path of l length from the moment of the photon entry into the medium along the given trajectory[11,13] (see Section 4).

2.3. Monte Carlo algorithms for calculation of the fluxes and brightness fields

In this section, the Monte Carlo algorithms, used for calculation of the radiative characteristics in the plane-parallel horizontally homogeneous atmosphere without taking into account the absorption by the atmospheric gases, are briefly described. They allow us to clearly show which modifications of the presented relations were used in simulating the solar radiative transfer in the spatially inhomogeneous and stochastic clouds and to account for the molecular absorption.

Before passing to the statistical simulation of the radiative characteristics, we transform the multi-component medium (aerosol and cloud particles and the molecular component of the atmosphere) to the medium with the extinction $\sigma(z)$ and scattering $\sigma_s(z)$ coefficients and with the scattering phase function $g(z, \mu)$ basing on the formulas

$$\begin{gathered}\sigma(z)=\sigma_{cl}(z)+\sigma_a(z)+\sigma_m(z),\ \sigma_m(z)=\sigma_R(z)+\varepsilon_m(z),\\ \sigma_s(z)=\sigma_{cl,s}(z)+\sigma_{a,s}(z)+\sigma_R(z),\\ g(z,\mu)=(\sigma_{cl,s}(z)g_{cl}(z,\mu)+\sigma_{a,s}(z)g_a(z,\mu)+\\ +\sigma_R(z)g_R(\mu)/\sigma_s(z).\end{gathered} \tag{13}$$

(In addition to these characteristics, we will use the notion of the single scattering albedo $\Lambda = \sigma_s(z)/\sigma(z)$). To construct the photon trajectories in the horizontally homogeneous medium with the optical characteristics (13), the canonical procedures of simulation of photon free-pathlength and direction are realized.[11–13,15,24]

To calculate upward $F^{\uparrow}(z^*)$ and downward $F^{\downarrow}(z^*)$ fluxes of solar radiation at the level $z = z^*$, the model uses the method of direct (analog) simulation[13]:

$$F^{\uparrow(\downarrow)}(z^*) = E_0 \sum_{i=1}^{N_{tr}} m_i / N_{tr}. \tag{14}$$

Here, N_{tr} is the number of photon trajectories; and m_i is the number of crossings by photon of the plane $z = z^*$ in the ith trajectory in the direction $\boldsymbol{\omega}$. It is assumed in calculations that the solar radiation flux is incident on the atmosphere top, $E_0 = 1$; in order to path to the absolute values, $F^{\uparrow(\downarrow)}(z^*)$ should be multiplied by $\pi S_\lambda |c_\odot|$.

In accordance with Eq. (11), the intensity of the scattered solar radiation $I_1(z^*, \boldsymbol{\omega}^*)$ at the level $z = z^*$ in a given direction $\boldsymbol{\omega} = \boldsymbol{\omega}^*$ represents a linear functional $I_1(z^*, \boldsymbol{\omega}^*) = (f, h_{z^*})$. To estimate it, we use the *weighting* method of local estimate (MLE) and the method of adjoin walks (MAW).

In the $I_1(z^*, \boldsymbol{\omega}^*)$ calculation by the method of local estimate, at each point of the photon collision $x_n = (\mathbf{r}_n, \boldsymbol{\omega}_{n-1})$, $\mathbf{r}_n = \mathbf{r}_{n-1} + \boldsymbol{\omega}_{n-1} l_n$ (l_n is the free-pathlength), the quantity $Q_n h'_{z^*}(\mathbf{x}_n, \boldsymbol{\omega}^*)$ is calculated (see Eq. (6)), where

$$Q_0 = \frac{1}{2\pi},\ Q_n = \begin{cases} Q_{n-1}\Lambda(z_n), & z_n \in (0, H] \\ Q_{n-1}A_s, & z_n = 0; \end{cases} \tag{15}$$

$$h'_{z^*}(\mathbf{x}_n, \boldsymbol{\omega}^*) = \begin{cases} g(z_n, \mu_{n-1})\exp\{-\tau(z^*, z_n)/c^*\}/|c^*|, (z^* - z_n)c^* > 0, z_n \in (0, H]; \\ 2\exp\{-\tau(z^*, z_n)/c^*\},\ c^* > 0,\ z_n = 0; \\ 0,\ (z^* - z_n)c^* < 0; \end{cases} \tag{16}$$

$$\mu_{n-1} = (\omega_{n-1}, \omega^*).$$

To calculate $I_1(z^*, \boldsymbol{\omega}^*)$ by the method of adjoin walks, the particle trajectory is simulated with the initial density $\delta(z - z^*)\delta[\boldsymbol{\omega} - (-\boldsymbol{\omega}^*)]$, and at each collision point the quantity $\psi_1(\mathbf{r}, \boldsymbol{\omega}) = \Phi_0(\mathbf{r}, -\omega)/\sigma(\mathbf{r})$ is calculated. The distribution density of initially scattered particles is

$$\begin{gathered}\Phi_0(z, \boldsymbol{\omega}) = \sigma_s(z) g(z, \mu)\exp\{-\tau(z, H)/c_\odot\}/2\pi, \\ \mu = (\boldsymbol{\omega}_\odot, \boldsymbol{\omega}).\end{gathered} \tag{17}$$

According to relations (10) and (17), in the framework of the MAW, at each point $\mathbf{x}_n$ the quantity $Q_n \psi'_1(\mathbf{x}_n)$, is calculated, where the weights Q_n are defined by formula (15), and

$$\psi_1'(\mathbf{x}_n)=\begin{cases} g(z_n,\mu_{n-1})\exp[-\tau(z_n,H)/|c_\odot|], & z_n\in(0,H]; \\ 2\exp(-\tau_0/|c_\odot|), & z_n=0. \end{cases} \quad (18)$$

The quantity $2\exp(-\tau_0/|c_\odot|)$, $\tau_0 = \tau(0, H)$, is calculated beyond the procedure of statistical simulation.

The MLE makes it possible to calculate the contribution from each collision point in estimation of I_1 for a large set of observation planes and viewing directions $\{\omega_{kj}^*=(\xi_k,\varphi_j)\}$, $k = 1, ..., N_\xi$; $j = 1, ..., N_\varphi$. When solving some problems (and, in particular in the calculations of the scattered radiation intensity in solar almucantar), the efficiency of the MAW can be increased, because the accounting for the atmosphere symmetry also allows estimation of a few functionals based on one simulated photon trajectory.[15] Let the azimuthal dependence of the downward radiation intensity be estimated for a specified $z = z^*$ and constant viewing zenith angle ξ_1 for a set of azimuth angles of detector φ_j, $j = 1, ..., N_\varphi$. Then, the photon trajectories, starting at the point $\mathbf{r}^* = (x, y, z^*)$ in the direction $-\boldsymbol{\omega}_1 = (-a_1, -b_1, -c_1)$, $a_1 = \sin\xi_1\cos\varphi_1$, $b_1 = \sin\xi_1\sin\varphi_1$, $c_1 = \cos\xi_1 \le 0$, can be used in estimation of intensity for the entire set of azimuth angles of detectors. To do this, it is necessary to pass from the set of the detector angles (ξ_1, φ_j) to the set of the solar angles $\boldsymbol{\omega}_{\odot,j} = (\xi_\odot, \varphi_{\odot,j})$ from Eq. (17):

$$a_{\odot,j} = \sin\xi_1\cos(\varphi_\odot + \varphi_1 - \varphi_j),$$

$$b_{\odot,j} = \sin\xi_1\sin(\varphi_\odot + \varphi_1 - \varphi_j),\ c_{\odot,j} = -\cos\xi_1.$$

The detailed recommendations concerning the expedience of the use of MLE and MAW for solution of most problems of atmospheric optics are given, e.g., in Ref. 15.

2.4. Testing of the Monte Carlo algorithms in the horizontally homogeneous plane parallel atmosphere

The testing of any algorithms is a necessary stage in their development and implementation. To do this, we compared our calculations with results obtained by other authors and presented in monograph of Lenoble.[25] In the testing, the model of molecular-aerosol atmosphere was used, in which the vertical behavior of aerosol optical characteristics corresponded to the model, recommended for radiation calculations in conditions of the cloudless sky.[16] Our data were brought to correspondence with simulation results[25] through multiplication by $\pi|c_\odot|$; the relative calculation error did not exceed 1%.

Since calculations of the radiation intensity,[25] made by different methods, well agree, we present only the comparison of our results with calculations based on the finite-difference method (FDM). Table 1 presents calculations of the transmitted radiation brightness at the surface level $I_1^\downarrow(z=0,\mu,\varphi)$, performed on the basis of two our algorithms (methods of local estimate and adjoin walks) and FDM for $A_s = 0$.

Table 1. Brightness of downward diffuse radiation at the surface level $z = 0$ as a function of cosine of viewing zenith angle μ. Urban aerosol,[16] λ = 0.55 μm; solar zenith angle $\xi_\odot = 60°$, $A_s = 0$

μ	Our calculations		Lenoble[25]
	MLE	MAW	FDM
	Azimuth angle of detector φ = 0°		
−1	0.0776	0.0778	0.0771
−0.8	0.2550	0.2560	0.2555
−0.4	0.5020	0.503	0.4716
	Azimuth angle of detector φ = 180°		
−1	0.0776	0.0773	0.0771
−0.8	0.0474	0.0475	0.0474
−0.4	0.0471	0.0471	0.0469

Calculations of downward diffuse radiation fluxes at the surface level $F_s^\downarrow(z=0)$ and reflected radiation at the atmosphere top $F^\uparrow(z = 30$ км$)$ are presented in Table 2.

Table 2. Fluxes of diffuse radiation at the surface level and at the atmosphere top. Continental aerosol,[16] solar zenith angle $\xi_\odot = 75°$, $A_s = 0$

Wavelength λ, μm	Our calculations		Lenoble[25]	
	$F_s^\downarrow(z=0)$	$F^\uparrow(z=30$ km$)$	$F_s^\downarrow(z=0)$	$F^\uparrow(z=30$ km$)$
0.4	0.318	0.36	0.317	0.362
0.55	0.292	0.221	0.284	0.218
1.06	0.148	0.078	0.143	0.076

It follows from the presented results that the disagreement in calculations does not exceed 1–3% and, hence, the suggested algorithms can be used for estimation of the brightness fields in the plane-parallel horizontally homogeneous atmosphere.

2.5. Multilayer clouds

In the presence of multilayer clouds, partly covering the sky, we use an approximate method of calculation of the radiative characteristics. The essence of the method is explained by the example of the calculation of upward and downward radiative fluxes in two-layer broken clouds.

Consider the model of the atmosphere, within which two layers are partly occupied by clouds. The $F^{\uparrow(\downarrow)}$ values at the level z are determined by the relation

$$F^{\uparrow(\downarrow)}(z)=K_{\text{clr=1,clr=2}}F^{\uparrow(\downarrow)}_{\text{clr=1,clr=2}}(z)+K_{\text{oc=1,clr=2}}F^{\uparrow(\downarrow)}_{\text{oc=1,clr=2}}(z)+$$

$$+K_{\text{clr=1,oc=2}}F^{\uparrow(\downarrow)}_{\text{clr=1,oc=2}}(z)+K_{\text{oc=1,oc=2}}F^{\uparrow(\downarrow)}_{\text{oc=1,oc=2}}(z), \quad (19)$$

where $F^{\uparrow(\downarrow)}_{\text{clr=1,clr=2}}$, $F^{\uparrow(\downarrow)}_{\text{oc=1,clr=2}}$, $F^{\uparrow(\downarrow)}_{\text{clr=1,oc=2}}$, $F^{\uparrow(\downarrow)}_{\text{oc=1,oc=2}}$ correspond to $F^{\uparrow(\downarrow)}$ values under conditions of the

clear sky ("clr"), overcast sky ("oc"), and one- and two-layer clouds. They are calculated based on 1*D* radiative transfer equation. The weights, with which they are combined, are determined by some or other hypothesis of the cloud overlap. From three most known hypotheses, namely, minimal, maximal, and random overlap (see, e.g., Ref. 26), the general circulation models (GCMs) commonly use the latter two or their combination. The combined scheme suggests the use of the hypothesis of the maximal overlap for contiguous cloud layers (e.g., cloud layers within one atmospheric level) and the hypothesis of random overlap for cloud layers, which do not meet (for clouds at different atmospheric levels). These hypotheses have no sufficient theoretical or empirical foundation and are selected for each GCM model due to the best correspondence of simulation results to satellite and ground-based observational data.

Let N_1 and N_2 be the cloud fractions in the first and second cloud layers, respectively. Then, the weights K_{ij} in formula (19) for hypotheses (hyp) of random (rand) and maximal (max) overlap are:

$$\begin{aligned} K^{\text{hyp}}_{\text{clr=1,clr=2}} &= \begin{cases} (1-N_1)(1-N_2), & \text{hyp = rand;} \\ 1-\max(N_1,N_2), & \text{hyp = max;} \end{cases} \\ K^{\text{hyp}}_{\text{oc=1,clr=2}} &= \begin{cases} N_1(1-N_2), & \text{hyp = rand;} \\ \max(0,N_1-N_2), & \text{hyp = max;} \end{cases} \\ K^{\text{hyp}}_{\text{clr=1,oc=2}} &= \begin{cases} (1-N_1)N_2, & \text{hyp = rand;} \\ \max(0,N_2-N_1), & \text{hyp = max;} \end{cases} \\ K^{\text{hyp}}_{\text{oc=1,oc=2}} &= \begin{cases} N_1N_2, & \text{hyp = rand;} \\ \min(N_1,N_2), & \text{hyp = max.} \end{cases} \end{aligned} \qquad (20)$$

Generalization of formulas (19)–(20) to the cases, when the number of the cloud layers exceeds two, is given, e.g., in Ref. 27.

3. Spatially inhomogeneous atmosphere

The presented algorithms for calculation of fluxes and brightness fields of solar radiation are developed for the model of the atmosphere, whose inhomogeneity is caused by the irregular shape of clouds, their sizes, position in the space, and fluctuations of the optical characteristics inside some individual cloud. The source of information on the spatially inhomogeneous two- (2*D*) and three-dimensional (3*D*) realizations of cloud fields, whose scale varies in the range from a few kilometers to a few hundreds of kilometers, are the data of satellite and ground-based observations, as well as "physical" and mathematical cloud models.

Most *physically based* cloud models are developed presently in the framework of the international Global Energy and Water Cycle Experiment (GEWEX) Cloud System Study (GCSS) Project, whose goal is to develop and test the physically based cloud parameterizations for models of weather and climate prediction.[28] From the viewpoint of the study of the finite-size cloud effects (3*D* effects), the results obtained in the framework of the Large Eddy Simulation (LES) models are most useful. They are designed for the study of thermodynamic parameters of the atmospheric boundary layer, overlaid by the stratocumulus or small cumulus clouds.[29–32] A brief overview of the mathematical cloud models and the relevant bibliography will be presented in the continuation of the present paper (Part II); therefore, we do not focus here on their description.

To calculate the radiation characteristics within realizations of inhomogeneous clouds, two methods are presently used, allowing the "exact" solution of the three-dimensional radiation transfer equation: the Monte Carlo method and a combination of methods of spherical harmonics and discrete ordinates. (The latter approach is realized in the form of Spherical Harmonic Discrete Ordinate Method (SHDOM) software package[33] and in the RADUGA radiation code[34]). Because of the complex spatial cloud structure and the need in taking into account of the radiation interaction with cloud particles, aerosol, atmospheric gases, and underlying surface, the problem of testing the radiation codes, both being in hand and being under development, becomes important.

This section describes the statistical algorithms, developed by the author for calculation of radiation characteristics in horizontally and vertically inhomogeneous clouds (radiation code IAOT, Institute of Atmospheric Optics, Tomsk); also, it presents the comparison of IAOT-based calculations of fluxes and brightness fields of solar radiation with results, obtained on the basis of other radiation codes in the framework of the international project "Intercomparison of 3*D*-Radiation Codes" (I3RC).[4] The presented algorithms[35,36] are designed for calculation of radiation characteristics in one- (1*D*), two- (2*D*), and three-dimensional (3*D*) cloud realizations. Their sources are data of satellite and ground-based observations, models of cloud formation, and LES models: the characteristic spatial resolution in such realizations is 30–100 m in horizontal and vertical directions.

3.1. Radiation code IAOT: algorithms for calculation of fluxes and brightness fields

One- and two-dimensional cloud realizations can be constructed based on the experimental data: in this case, as a rule, they are determined by the spatial distribution of the optical depth $\tau(\mathbf{r})$ and height of the top $H_{\text{cl}}^{\text{top}}(\mathbf{r})$ and bottom $H_{\text{cl}}^{\text{bot}}(\mathbf{r})$ cloud boundaries.

Realization of type 1 is a 1*D*-model (*X*). Heights of the top and bottom boundaries are constant throughout the cloud field; the optical depth depends on only one coordinate x and is constant within each of the N_x pixels $x_i \le x \le x_{i+1}$: $\tau(x) = \tau_i$, $i = 1, \ldots, N_x$. The horizontally-

inhomogeneous cloud is assumed to be infinite in the direction of OY axis (Fig. 2*a*).

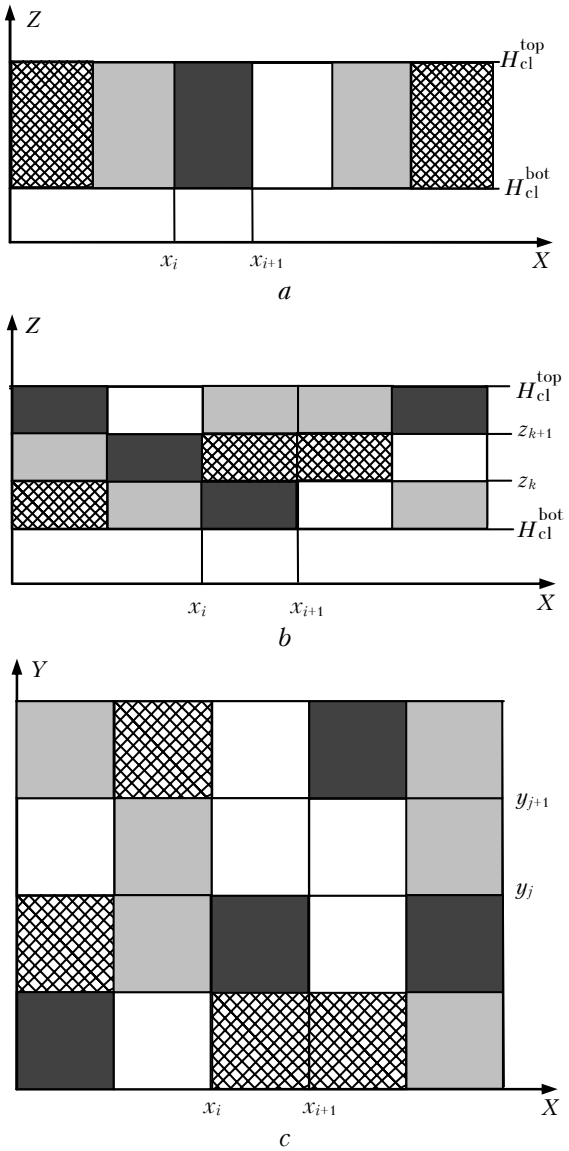

Fig. 2. Schematic illustration of type 1 (*a*), type 2a (*b*), and type 2b (*c*) realizations. Different colored rectangles correspond to the pixels with different optical depths.

Realization of type 2a is a 2*D* model (*XZ*). In contrast to the 1*D* model, the pixel is considered as a band infinite in the direction of the OY axis $(x_i, x_{i+1}) \times (z_k, z_{k+1})$, $i = 1, ..., N_x$; $k = 1, ..., N_z$. In this realization, a column of width $x_i \le x \le x_{i+1}$ is presented in the form of a set of cells, located one above another, each with geometrical and optical thicknesses $(z_{k+1} - z_k)$ and $\tau_{i,k}$, respectively. The heights of the top and bottom boundaries of the ith column $x_i \le x \le x_{i+1}$ may vary: $H_{cl}^{top}(x) = H_{cl,i}^{top}$, $H_{cl}^{bot}(x) = H_{cl,i}^{bot}$; in this case, the cloud field is characterized by irregular top and bottom boundaries. On the whole, $H_{cl}^{top} = \max_i H_{cl,i}^{top}$, and $H_{cl}^{bot} = \min_i H_{cl,i}^{bot}$ are considered as the top and bottom boundaries of the cloud field (Fig. 2*b*).

Realization of type 2b is a 2*D* model (*XY*). The optical depth and the height of cloud top boundary depend on the coordinates x and y:

$$\tau(x, y) = \tau_{i,j}, \; H_{cl}^{top}(x,y) = H_{cl,i,j}^{top}$$

within

$$(x_i, x_{i+1}) \times (y_j, y_{j+1}), \; i = 1, ..., N_x; \; j = 1, ..., N_y.$$

The height of the bottom boundary of clouds in this realization is, as a rule, constant (Fig. 2*c*).

Realization of type 3: three-dimensional cloud realizations 3*D* (*XYZ*) are constructed in the framework of LES models or cloud formation models; the extinction coefficient does not change within the pixel $(x_i, x_{i+1}) \times (y_j, y_{j+1}) \times (z_k, z_{k+1})$, $i = 1, ..., N_x$, $j = 1, ..., N_y$, $k = 1, ..., N_z$; and the heights of the top and bottom boundaries of the cloud layer may vary within the simulation domain.

In realizations of types 1 and 2, the extinction coefficient σ_{cl} within each subregion is assumed to be constant. It is calculated based on the specified values of the optical and geometrical pixel thicknesses. In addition to the cloud extinction coefficient, within each pixel the single scattering albedo and scattering phase function are also specified. (The two last cloud optical characteristics in the IAOT code were assumed constant throughout the cloud field.) The cloud realization belongs to one of the layers of the plane parallel model of the atmosphere $H_{cl}^{bot}(x,y) \le z \le H_{cl}^{top}$. The distribution of aerosol optical characteristics, as well as Rayleigh scattering and molecular absorption coefficients within all (including cloudy) atmospheric layers are assumed to be horizontally homogeneous (1*D* model). The reflection from the underlying surface is simulated in accordance with the Lambert law; and the underlying surface is assumed to be horizontally homogeneous.

For calculation of solar radiation fluxes, we used the method of direct simulation (14). The intensity of upward and downward diffuse radiation $I_1(z^*, \boldsymbol{\omega}^*)$ at the level z^* in direction $\boldsymbol{\omega}^*$ was calculated using the MLE according to formulas (15) and (16), in which the optical pathlength $\tau(\mathbf{r}_{out}, \mathbf{r}^*)$ in direction $\boldsymbol{\omega}^*$ is defined by the relation

$$\tau(\mathbf{r}_{out}, \mathbf{r}) = \left| \int_z^{z^*} \sigma(\mathbf{r}') dz' \Big/ c^* \right|, \; \mathbf{r}' = \mathbf{r} + (\xi - z)/c^*.$$

The molecular absorption in the IAOT code at the given stage is taken into account through the single scattering albedo (see Section 4).

In the medium with varying extinction coefficient $\sigma(\mathbf{r})$, the most difficult step in the photon trajectory modeling is the procedure of the *free-pathlength* simulation. If the medium represents a set of small subregions with constant extinction

coefficient (just this situation is in case of cloud realizations with an above-mentioned spatial resolution of 30–100 m), then the increase of computer time for simulation of l is associated with time consumptions required for simulation of distances to the boundaries of the corresponding subregions. In the IAOT code, we used the maximal cross-section method for simulation of free pathlength, which, from the viewpoint of computer implementation, is one of the simplest.[11,12]

Concerning the procedure of simulation of the particle travel direction, note that the aerosol and cloud scattering phase functions in the IAOT code are specified in the form of tables, calculated beyond the procedure of the statistical simulation. In a number of cases (see subsection 3.2) we used the Henyey–Greenstein phase function as the scattering phase function

$$g_{HG}(\mu) = (1-\langle\mu\rangle^2)/(1+\langle\mu\rangle^2 - 2\langle\mu\rangle\mu)^{3/2},$$

where $\langle\mu\rangle$ is the mean cosine of the scattering angle θ (asymmetry factor). In this situation, for simulation of $\mu = \cos\theta$ it is reasonable to use the formula[37]:

$$\mu = [1 + \langle\mu\rangle^2 - ((\langle\mu\rangle^2 - 1)/(2\langle\mu\rangle\alpha - \langle\mu\rangle - 1))^2]/(2\langle\mu\rangle).$$

Here, $0 \le \alpha \le 1$ is a random number.

Note in conclusion of the Section that algorithms of the IAOT code are realized so that to perform calculations simultaneously for different values of single scattering albedo Λ of the medium and surface albedo A_s, and also to save the calculated results after completion of each package operation into some intermediate file, offering the possibility to continue the calculations until reaching the required accuracy. Such a computation scheme substantially improves the efficiency of the used statistical algorithms. Moreover, the calculation of the radiation characteristics can be readily extended to cases, when 1) the underlying surface is not horizontally homogeneous and/or the radiation reflection from it is described by the law other than Lambert law, and 2) all optical characteristics of the medium (not only the extinction coefficient) vary from one pixel to another. Naturally, this leads to increase of computer time, however allowing one, if necessary, to take into account most fully the variations of the optical characteristics of the atmosphere and underlying surface.

3.2. Comparison of the algorithms of calculation of radiative characteristics in 3D clouds

This section describes the comparison results of calculations, performed with different radiation codes in the course of implementation of the international Project I3RC.[4] The goal of the I3RC Project (Responsible NASA Official: Robert Cahalan, GSFC, NASA, USA; http://i3rc.gsfc.nasa.gov) is:

– to improve current algorithms, used to calculate the radiative characteristics in 3*D* inhomogeneous clouds;

– to develop efficient approximations, useful for development of climate models; and

– to develop widely accessible radiation codes for description of radiative transfer in the cloudy atmosphere in the UV, visible, and near IR spectral regions.

The implementation of the I3RC Project involved 3 stages, two of which are now successfully completed (the list of participants of the stage I, methods of calculations, and extension names of the radiation codes are presented in Table 3). At each step, a set of the cloud realizations, described below, was proposed to the I3RC participants. It was assumed that the boundary conditions along OX and OY axes were periodic, and that the cloud top boundary was illuminated by the solar radiation flux F_0 in the direction $\omega_\odot$. In each of the realizations, it was necessary to calculate three first moments of the albedo R, transmission T, absorption A, and horizontal transfer $H = 1 - T(1 - A_s) - A$, as well as the reflectivity I_u and transmittance I_d of the layer:

$$I_{u(d)} = \pi I^{\uparrow(\downarrow)}/(F_0|c_\odot|),$$

where $I^{\uparrow(\downarrow)}$ is the scattered radiation intensity at nadir (zenith) at the level of the cloud top (bottom) boundary (see for details http://i3rc.gsfc.nasa.gov). The calculations were performed at different values of A_s, solar zenith angle $\xi_\odot$, single scattering albedo Λ, and scattering phase functions.

I3RC: phase I. For the I3RC phase I, three cloud realizations were selected.

Case 1 represents the simplest cloud field and corresponds to the realization of type 1. The calculations assumed: $N_x = 32$; the optical depth τ equal to 2 for the first 16 pixels and to 18 for other pixels; the geometrical thickness H of the cloud field equal to 0.25 km; the extent of the cloud field along the OX axis, L_x equal to 0.5 km.

In *case 2*, the cloud realization (realization of type 2a) was constructed using Millimeter cloud radar (MMCR) and Microwave radiometer (MWR) measurements, performed at the Atmospheric Radiation Measurement – Cloud and Radiation Test Bed (ARM-CART) site (Lamont, OK) in February, 1998 (the data were provided by K.F. Evans). It was assumed that the field consisted of 640 pixels along OX axis (32 km) and 54 pixels along OZ axis, with horizontal and vertical resolutions of 50 and 45 m, respectively.

Case 3 used the cloud realization, retrieved from LANDSAT data and provided by B. Wielicki (realization of type 2b, Figs. 3*a* and *b*). It was assumed in calculations that $N_x = N_y = 128$, and the horizontal resolution was 30 m along each axis. All cases of the I3RC phase I disregarded the radiation interaction with aerosol and atmospheric gases.

Table 3. List of participants of phase I of the I3RC project (based on materials of Cahalan et al.[4])

Code	Institution	Institution representatives	Method of calculation
ARIZ (USA)	University of Arizona	M. Garay, R. Davies	Monte Carlo
COLS (USA)	Colorado State University	P. Patrain	Monte Carlo
IAOT (Russia)	Institute of Atmospheric Optics	T. Zhuravleva	Monte Carlo
KIAE1, KIAE2 (Russia)	Kurchatov Institute	A. Rublev	Monte Carlo, method of adjoin walks
LANL1, LANL2, LANL3 (USA)	Los Alamos National Laboratory	A. Davis	3D delta-Eddington diffusion model, DA (Discrete angle), TWODANT (Two-dimensional diffusion-accelerated neural-particle transport)
MESC1, MESC2 (Canada)	Meteorological service of Canada	H. Barker	Monte Carlo, Monte Carlo (delta-scaled optical properties)
NCAR (USA, now Germany), now DZLR	National Center for Atmospheric Research	B. Mayer	Monte Carlo
PENN (USA)	The Pennsylvania State University	E. Clothiaux	Monte Carlo
PNNL (USA)	Pacific Northwest National Laboratory	E. Kassianov	Monte Carlo
UCOL (USA)	University of Colorado	K.F. Evans	SHDOM
UCSB (USA)	University of California, Santa Barbara		Monte Carlo
UMBC1, UMBC2 (USA)	University of Maryland, Baltimore County (UMBC)	A. Marshak, T. Varnai	Monte Carlo
UMBC3, UMBC4 (USA)	University of Maryland, Baltimore County (now Max Plank Institute)	S. Kinne	Monte Carlo, DA (six-beam discrete-space model)
UNBP1, UNBP2 (France)	Universite Blaise Pascal	F. Szczap	Neural networks, NIPA (Nonlocal independent pixel approximation)
UNIK (Germany)	University of Kiel	A. Macke	Monte Carlo

Since it was impossible to obtain the standard radiation characteristics by statistical algorithms and SHDOM for involved cloud realizations, the goal of the comparisons was in finding the range of discrepancies, caused by the use of different codes, and in understanding the cause of their arise. (An analogous approach was used in inter-comparison of GCM radiation codes.[38]) In phase I, the spatial distributions and the domain-average radiation characteristics were compared, as well as the cross correlations and root-mean-square deviations were calculated with respect to computations by the participating code UMBC1 (University of Maryland, Baltimore County).

The results, obtained with use of UMBC1, were considered as the reference, because this code was developed by GSFC-UMBC, the institution, which conducted a joint analysis of results; moreover, UMBC1 could be used in the comparison procedure before publishing the obtained results.

The comparison of the results of I3RC participants for all suggested cases are compared at the project site http://i3rc.gsfc.nasa.gov. This paper presents the spatial distribution of the cloud reflectivity $I_u(x, y)$ for the case 3 (Fig. 3*c*) as an example.

All data presented in this figure were obtained by the Monte Carlo method. The $I_u(x, y)$ variations (from one code to another) were caused primarily by the different number of photons, used in the calculations, whereas domain-average values of the reflectivity $\overline{I}_u$ nearly coincided even for the most "noisy" brightness fields. We note that the mean $\overline{I}_u$, calculated in the Independent Pixel Approximation (IPA), differs weakly from the calculations of participants of I3RC phase I, whereas the spatial distribution $I_{u,\mathrm{IPA}}(x, y)$ is much smoother than the Monte Carlo calculations.[4]

As to the IAOT code, the analysis of results has shown that the correlation coefficient between the radiative characteristics, calculated with IAOT and UMBC1 codes, exceeded 99%.

I3RC: phase II. For this phase, realizations of convective and stratocumulus clouds, obtained with the use of LES models, were used.

Realization for *case 4* was provided by B. Stevens, who modeled small continental cumulus clouds using data of experiments at the ARM Oklahoma site.[32] The cloud field consisted of $100\times100\times36$ cells with a grid size of $66.7\times66.7\times40$ m; in accordance with the modeling results, the cloud amount was 0.23; mean and maximal values of liquid water path LWP and optical depth were 38.2 (1141) g/m^2 and 6.03 (150.5), respectively. The stratocumulus cloud field (*case 5*) was obtained by C.-H. Moeng using data of the FIRE-I experiment.[29]

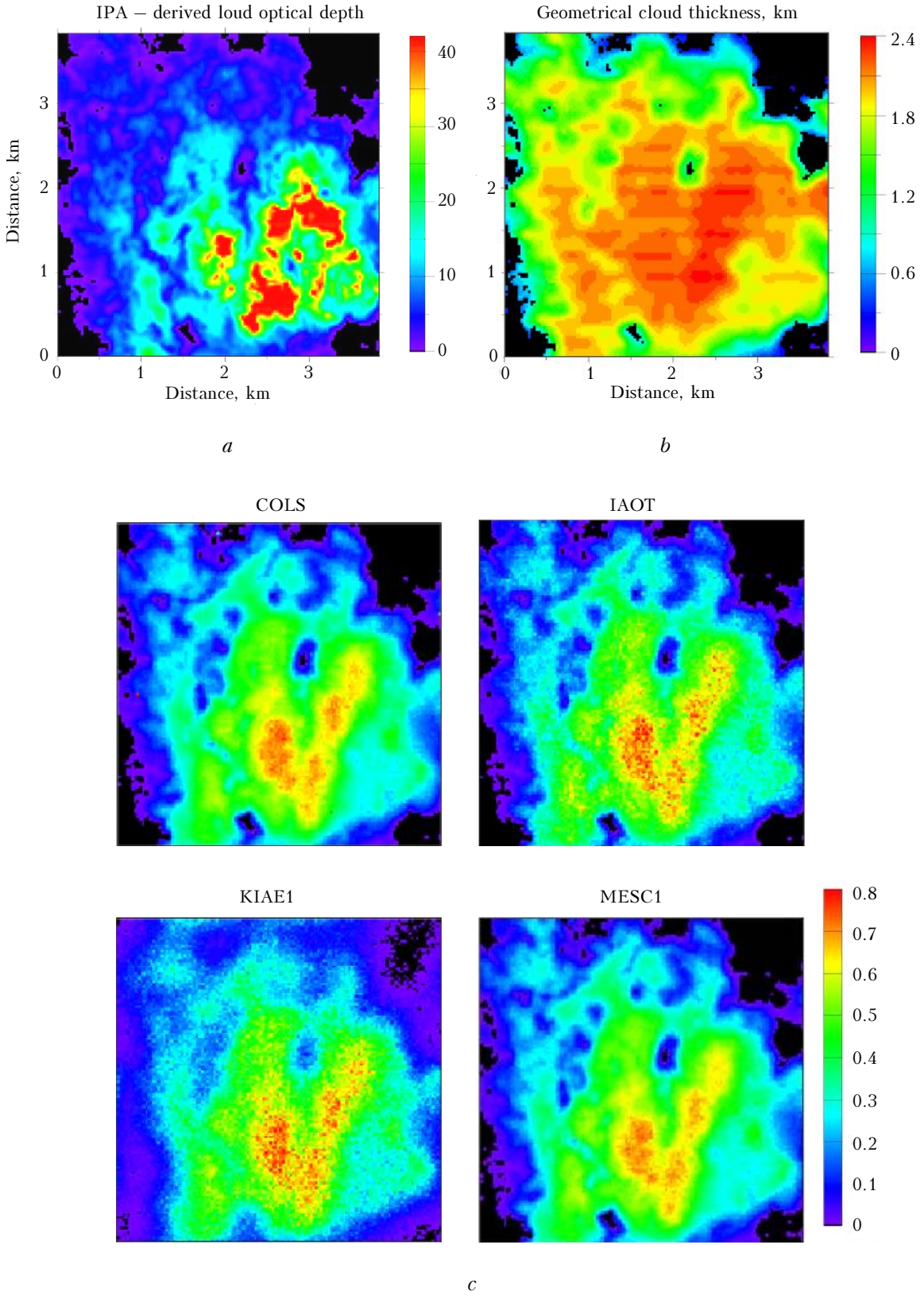

Fig. 3. Spatial distribution of cloud optical (*a*) and geometrical (*b*) thicknesses and reflectivity of the cloud layer (*c*). Case 3 of I3RC project, phase I: solar zenith angle $\xi_{\odot} = 60°$, $\Lambda = 0.99$.

Almost overcast cloud field (cloud amount of 0.9) was represented by 64×64×17 cells with a grid size of 55×55×25 m and was more homogeneous than in the case 4; mean and maximal values of LWP and optical depth were 51.6 (263) g/m^2 and 7.13 (27.3), respectively (Fig. 4*a*).

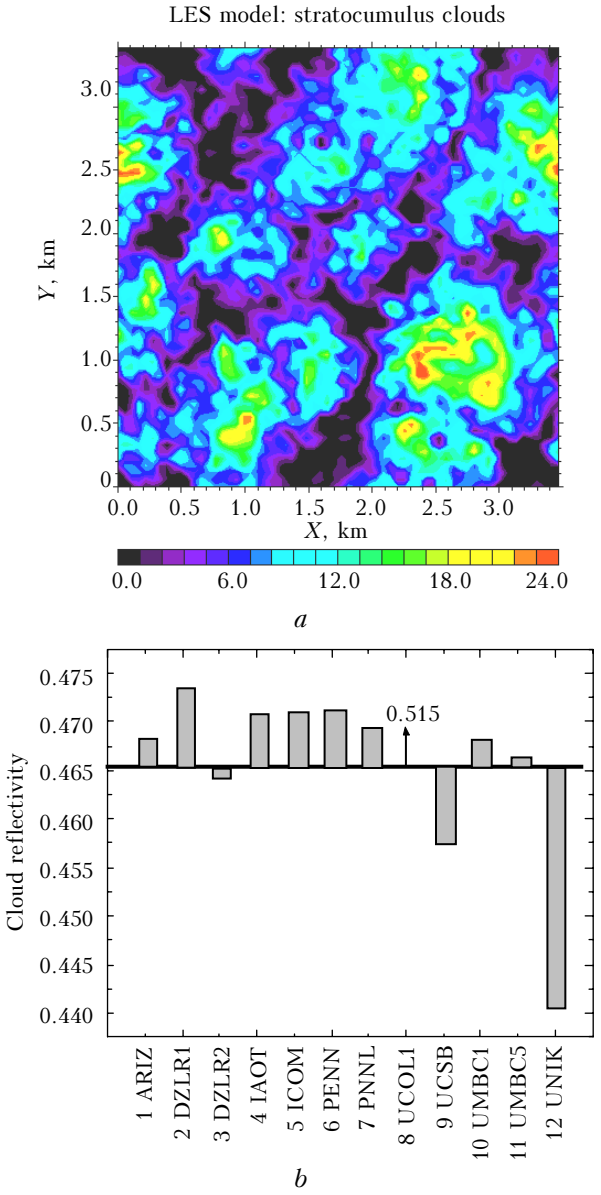

Fig. 4. Spatial distribution of optical depth (*a*) and cloud reflectivity I_u (*b*) averaged over the simulation domain. Case 5 of I3RC phase II: scattering phase function of $C1$ cloud ($\lambda = 0.67$ μm), $\xi_\odot = 0°$. The horizontal line corresponds to the mean I_u value (equal to 0.4653) of all participating codes. For extension names of the radiation codes, see Table 3.

The phase II focused on calculation of monochromatic brightness fields and heating/cooling rates. In contrast to the phase I, the numerical experiments allowed for the presence of aerosols and atmospheric gases, as well as the effects of anisotropy (non-Lambertianity) of the underlying surface. As the reference ("true") values of the radiative characteristics, the averaged results of all I3RC participants, submitted results in phase II, were taken. The example, presented in Fig. 4*b*, shows a good agreement of the domain-average reflectances of the cloud field, which were calculated with the use of different codes, including IAOT, which was used only for calculation of the cloud reflectance. Such an agreement is also typical for other numerical experiments implemented in the second phase of the comparisons.

Accuracy of calculations. In the I3RC phase I, computers Pentium (120 MHz) and Pentium II (450 MHz) were used in calculations.[35,36] Table 4 presents data on the number of photons and calculation errors in radiation characteristics: mean pixel level error (MPLE) and mean error for entire simulation domain, (ME).

In *case 1*, 50 million photons were used for simulation, i.e., an average of 1.56 million of photons incident on the top of each pixel. Since the cloud realization, corresponding to this case, is quite simple, the given number of photons was sufficient to ensure the calculation accuracy for the spatial distribution of the radiative characteristics within 0.15% for R and T and 0.4% for $I_{u(d)}$.

Table 4. The number of photons and mean error in radiation calculations at the pixel level, MPLE, and in entire simulation domain, ME, for the cases 1–3 of I3RC project phase I. Experiment numbers correspond to different sets of input cloud parameters and illumination conditions (see http://i3rc.gsfc.nasa.gov for more detail)

Case	Experiment	R, T		$I_{u(d)}$	
		Number of photons, $\times 10^6$	MPLE/ME, %	Number of photons, $\times 10^6$	MPLE/ME, %
1	1–4	50	0.15/0.02	50	0.37/0,07
2	1–5	300	0.30/0.01	200	0.7/0.03
	6–8	200	0.35/0.01	100	2.5/0.12
3	1–4	500	1.1/0.01	500	1.8/0.02

In *case 2*, the number of photons incident on the top boundary of each pixel was, on the average, 460 thousands for experiments 1–5 and 310 thousands for experiments 6–8. (The experiments differ in the value of single scattering albedo and cloud scattering phase function, as well as in the surface albedo). The relative calculation error for the mean fluxes R and T was ≈ 0.3%. In the radiance calculations in the experiments 6–8 (the scattering phase function corresponded to the $C1$ cloud type), the number of photons at the top of each pixel was equal approximately to 156 thousands; therefore, the relative error of $I_{u(d)}$ calculation reached ≈ 2.5%. A feature of the cloud realization in *case 3* was a strong variation of the optical depth $\tau(x, y)$. Therefore, even for a quite large number of photons (500 millions for

domain as a whole, and 30 thousands per pixel), the MPLE was approximately 1.1% for fluxes and 1.8% for brightnesses (in directions to nadir and zenith).

By now, two I3RC phases have been successfully completed. Joint analysis of results has shown that the spatial distributions and domain-average radiation characteristics, obtained by different codes, mostly well correspond to each other. The project implementation, in particular, has yielded the calculations, which can be used as tests for the radiation codes (including those based on the approximate methods) in complex vertically and horizontally inhomogeneous media, as well as revealed the errors in the algorithms of the I3RC participants. There are strong grounds for believing that the I3RC results will be useful for solution of the problems relating to weather and climate prediction and for remote atmospheric sensing.

4. Accounting for the molecular absorption

The molecular absorption within a narrow spectral interval $\Delta\lambda$ is taken into account in our algorithms by means of two traditional approaches: with the use of the transmission function $T_{\Delta\lambda}(l)$ and through the probability of photon survival. Describe them briefly in the context of horizontally homogeneous model of the atmosphere.

4.1. Accounting for the molecular absorption on the basis of transmission function

Approach to accounting for the molecular absorption through *the transmission function* is based on the idea of time separation of the events: 1) molecular absorption and 2) scattering and absorption by cloud and aerosol particles.[13,39] The approach essence is as follows.

Let us represent $\Phi(\lambda, z, \omega)$ in the form

$$\Phi(\lambda,z,\omega) = \int_0^\infty J(\lambda,z,\omega,l)\mathrm{d}l,$$

where $J(\lambda, z, \omega, l)$ is the density of the number of particles scattered over the pathlength without taking into account the molecular absorption. If there was the absorption interaction described by the function $T(\lambda, l)$ on the path l, the density of the particle flux with accounting for the molecular absorption is

$$\Phi^{(\mathrm{m})}(\lambda,z,\omega) = \int_0^\infty J(\lambda,z,\omega,l)T(\lambda,l)\mathrm{d}l. \qquad (21)$$

Integration of Eq. (21) within the spectral interval $\Delta\lambda$ under the assumption that variations of the cloud and aerosol optical characteristics, as well as the Rayleigh scattering coefficients can be neglected [$J(\lambda, z, \omega, l) = J(z, \omega, l)$], yields:

$$\Phi^{(\mathrm{m})}_{\Delta\lambda}(z,\omega)=\frac{1}{\Delta\lambda}\int_{\lambda_1}^{\lambda_2}\Phi^{(\mathrm{m})}(\lambda,z,\omega)\mathrm{d}\lambda=$$

$$=\int_0^\infty J(z,\omega,l)\frac{1}{\Delta\lambda}\int_{\lambda_1}^{\lambda_2}T(\lambda,l)\mathrm{d}\lambda\mathrm{d}l=\int_0^\infty J(z,\omega,l)T_{\Delta\lambda}(l)\mathrm{d}l. \qquad (22)$$

Equation (22) provides for the method of calculation of the radiative characteristics by taking into account the absorption by the atmospheric gases through the transmission function $T_{\Delta\lambda}$. The photon trajectories are simulated in the medium without accounting for the molecular absorption, i.e., the extinction coefficient is defined by the formulas

$$\sigma(z) = \sigma_{\mathrm{cl}}(z) + \sigma_{\mathrm{a}}(z) + \sigma_R(z) - \text{within the cloud layer},$$

$$\sigma(z) = \sigma_{\mathrm{a}}(z) + \sigma_R(z) - \text{outside the cloud layer}. \qquad (23)$$

In the brightness calculation by the local estimate method, the pathlength is summed up from the atmosphere top to the collision point $\mathbf{r}_n$:

$$l^{(n)} = \sum_{k=1}^{n} l_k,\ l_k = |\mathbf{r}_k - \mathbf{r}_{k-1}|. \qquad (24)$$

In accordance with Eq. (6), the quantity $Q_n h'_{z^*}(\mathbf{x}_n,\omega^*)T_{\Delta\lambda}(l^{(n)}+l)$, is calculated at $\mathbf{r}_n$, where $l = |z_n - z^*|/|c_n|$ is the distance from $\mathbf{r}_n$ to the plane $z = z^*$ along the direction ω_n, while the weights Q_n and the function $h'_{z^*}(\mathbf{x}_n,\omega^*)$ are defined by the formulas (15) and (16), respectively. The analogous approach is also used in the brightness calculations by the *method of adjoin walks* with the only difference that the pathlength is measured from the point of the photon exit from the detector, while l is the distance from the collision point $\mathbf{r}_n$ to the atmosphere top in the direction $-\omega_\odot$.

Note that the density of the particle pathlength distribution $J(\lambda, z, \omega, l)$ can be calculated beforehand in the form of l histograms. It is important that the same histograms can be used in calculations of the radiative characteristics for diversity of situations, differing in the vertical profiles and concentrations of atmospheric gases, all other parameters of the atmosphere, underlying surface, and observation conditions being fixed.

In calculation of the radiative fluxes at the level $z = z^*$ by the method of direct simulation, we used the statistical estimate of the type (14): $\left(\sum_{i=1}^{N_{\mathrm{tr}}}\sum_{j=1}^{m_i}T_{\Delta\lambda}(l_{ij})\right)/N_{\mathrm{tr}}$, where l_{ij} is the photon pathlength in the ith trajectory from the point at the atmosphere top to the crossing of the level $z = z^*$ by the jth photon.[13]

The above-described method of accounting for the molecular absorption does not depend on the form of the transmission function. In the

implementation of our algorithms, we used two parameterizations of $T_{\Delta\lambda}$:

1) as a function of the absorbing mass w^* (see, e.g., Refs. 40–42):

$$T_{\Delta\lambda}(w^*) = \exp\left[-\beta_{\Delta\lambda}(w^*)^{m_{\Delta\lambda}}\right],$$

$$w^* = m\int_{z_1}^{z_2}\rho(z)[p(z)/p_0]^{n_{\Delta\lambda}}\,dz,$$

where $\rho(z)$ is the concentration of a fixed atmospheric gas; $p(z)$ is the atmospheric pressure at the height z; $p_0 = 1$ atm; m is the optical mass of the atmosphere in the direction ω, equal to $1/\cos\xi$ in the approximation of the plane parallel atmosphere; and the coefficients $\beta_{\Delta\lambda}$, $m_{\Delta\lambda}$, and $n_{\Delta\lambda}$ are the empirically determined constants;

2) in the form of a finite exponential series (k-distribution method[43,44]), when $T_{\Delta\lambda}$ in the case of the unscattered radiation is represented as

$$T_{\Delta\lambda}(m) = \int_0^1 \exp\left(-m\int_0^{H_{\text{atm}}}\kappa(\chi,z)\mathrm{d}z\right)\mathrm{d}g =$$

$$= \sum_{i=1}^{N_{\text{exp}}} C_i \exp\left(-m\int_0^{H_{\text{atm}}^{\text{top}}}\kappa(\chi_i,z)\mathrm{d}z\right),$$

where $\kappa(\chi, z)$ is the effective absorption coefficient in the space of cumulative frequencies χ, χ_i; C_i are the nodes and the coefficients of the Gaussian quadratures; $\sum_{i=1}^{N_{\text{exp}}} C_i = 1$.

4.2. Accounting for the molecular absorption on the basis of photon survival probability

In the case when the transmission function is parameterized in the form of exponential series, the molecular absorption can be accounted for through the probability of photon survival during the collision event. In accordance with the k-distribution method (see, e.g., Ref. 44), the flux density with accounting for the molecular absorption, $\Phi_{\Delta\lambda}^{(\text{m})}(\mathbf{x})$, can be written in the form

$$\Phi_{\Delta\lambda}^{(\text{m})}(\mathbf{x}) = \sum_{i=1}^{N_{\text{exp}}} C_i \Phi^{(m)}(\mathbf{x},\chi_i), \qquad (25)$$

where $\Phi^{(\text{m})}(\mathbf{x}, \chi_i)$ is related to the collision density $f^{(\text{m})}(\mathbf{x}, \chi_i)$ in the medium with extinction coefficient $\sigma(\mathbf{r}) + \kappa(\chi_i)$ by the formula

$$\Phi^{(\text{m})}(\mathbf{x},\chi_i) = f^{(\text{m})}(\mathbf{x},\chi_i)/[\sigma(\mathbf{r}) + \kappa(\chi_i)].$$

The collision density $f^{(\text{m})}(\mathbf{x}, \chi_i)$ satisfies the equation

$$f^{(\text{m})}(\mathbf{x},\chi_i) = \int_X k_i(\mathbf{x}',\mathbf{x}) f^{(\text{m})}(\mathbf{x}',\chi_i)\mathrm{d}\mathbf{x}' + \psi_i(\mathbf{x}), \quad (26)$$

where the kernel of the equation $k_i(\mathbf{x}', \mathbf{x})$ and distribution density of the sources $\psi_i(\mathbf{x})$ are equal, respectively, to

$$k_i(\mathbf{x}',\mathbf{x}) = [\sigma(\mathbf{r}) + \kappa(\mathbf{r},\chi_i)]\sigma_s(\mathbf{r}')g[\mathbf{r}',(\omega',\omega)]\times$$

$$\times\exp\{-\tau_0(\mathbf{r}',\mathbf{r}) - \tau_m(\mathbf{r}',\mathbf{r},\chi_i)\}\delta\{\omega - (\mathbf{r}-\mathbf{r}')/|\mathbf{r}-\mathbf{r}'|\}/$$

$$/[2\pi[\sigma(\mathbf{r}') + \kappa(\mathbf{r}',\chi_i)]|\mathbf{r}-\mathbf{r}'|^2]; \qquad (27)$$

$$\psi_i(\mathbf{x}) = [\sigma(\mathbf{r}) + \kappa(\mathbf{r},\chi_i)]\exp[-\tau(\mathbf{r}_0,\mathbf{r}) - \tau_m(\mathbf{r}_0,\mathbf{r},\chi_i)]\times$$

$$\times\delta(\omega - \omega_\odot).$$

Thus, the formulas (25)–(27) define the algorithm of calculating $\Phi_{\Delta\lambda}^{(\text{m})}(\mathbf{r}, \omega)$:

– for all $1 \le i \le N_{\text{exp}}$, the radiative transfer equation (26) is solved; the scattering coefficients of the medium are assumed unchanged for all i in each jth layer:

$$\sigma_s(z) = \sigma_{\text{cl,s}}(z) + \sigma_{\text{a,s}}(z) + \sigma_R(z) - \text{within the cloud layer},$$
$$\sigma_s(z) = \sigma_{\text{a,s}}(z) + \sigma_R(z) - \text{outside the cloud layer}, \qquad (28)$$

whereas the extinction coefficients of the medium at each ith step vary in accordance with the formula

$$\sigma(z) = \sigma_{\text{cl}}(z) + \sigma_{\text{a}}(z) + \sigma_R(z) + \kappa(z,\chi_i) -$$
$$\text{within the cloud layer}, \qquad (29)$$
$$\sigma(z) = \sigma_{\text{a}}(z) + \sigma_R(z) + \kappa(z,\chi_i) - \text{beyond the cloud layer};$$

the absorption by atmospheric gases is accounted for in each photon collision through the photon survival probability based on relations (28)–(29); and

– the obtained $\Phi^{(\text{m})}(\mathbf{x}, \chi_i)$ values are summed up with the corresponding weights in accordance with formula (25).

Obviously, for calculation of the radiation characteristics on the basis of the above approach, it is unnecessarily to use the Monte Carlo method: the RTE can be solved by any possible method for N_{exp} atmospheric situations, differing in profiles of the absorption coefficient $\kappa(z, \chi_i)$, $i = 1, \ldots, N_{\text{exp}}$. This is an advantage of the method, which accounts for the molecular absorption through the photon survival probability. Otherwise, if the radiation calculations are based on statistical algorithms (as in our case), the consumptions of the computer time depend proportionally on N_{exp} and the molecular absorption can be taken into account more efficiently through the use of the transmission function of the atmospheric gases.

In order to improve the description of the molecular absorption, in the development of our algorithms we tried to assimilate best the continuously updated spectroscopic information. To do this, the transmission function $T_{\Delta\lambda}$ was approximated by a finite exponential series; the effective molecular absorption coefficients were calculated for particular realizations of vertical profiles of the pressure, temperature, and concentration of different atmospheric gases, taking into account the instrumental function of the device and spectral behavior of the solar constant on the basis of different versions of HITRAN database. (This part of the work was done by K.M. Firsov).[46,47]

To test the algorithms, we compared two above-mentioned approaches to accounting for the molecular absorption: through the transmission function and through the photon survival probability; they were compared both to one another and to standard line-by-line calculations by B.A. Fomin.[47] The relative difference in the solar radiative fluxes in the chosen 500 cm^{-1} wide spectral intervals of the molecular-aerosol atmosphere did not exceed 1% in most cases (depending on the number of terms in the exponential series and on the HITRAN version). The comparison of model-based and measured spectral fluxes and brightness fields in the clear atmosphere and in the presence of horizontally homogeneous overcast clouds is given in Refs. 48 and 49. The results of the comparisons confirm the adequacy of our algorithms from the viewpoint of accounting for the molecular absorption.

When going to individual realizations of inhomogeneous clouds, the essence of the above approaches to accounting for the molecular absorption does not change. Thus, they can be used in radiation calculations, taking into account 3*D* effects of clouds (see also Refs. 35, 37, and 50).

Note in conclusion that for solution of a number of direct and inverse problems under clear-sky conditions, we implemented algorithms for calculating diffuse radiation fields by the method of adjoin walks in the spherical model of the atmosphere, taking into account the molecular absorption.[46,51]

This work was partially supported by the Russian Foundation for Basic Research (Grant No. 06-05-64484).

References

1. H. Barker, G.L. Stephens, P.T. Partain, J.W. Bergman, B. Bonnel, K. Kampana, E.E. Clothiaux, S. Clough, S. Cusack, J. Delamere, J. Edwards, K.F. Evans, Y. Fouquart, S. Freidenreich, V. Galin, Y. Hou, S. Kato, J. Li, E. Mlawer, J.-J. Morcrette, W. O'Hirok, P. Raisanen, V. Ramaswamy, B. Ritter, E. Rozanov, M. Schlesinger, K. Shibata, P. Sporyshev, Z. Sun, M. Wendisch, N. Wood, and F. Yang, J. Climate **16**, No. 16, 2676–2699 (2003).
2. S.A. Clough, M.W. Shephard, E.J. Mlawer, J.S. Delamere, M.J. Iacono, K. Cady-Pereira, S. Boukabara, and P.D. Brown, J. Quant. Spectrosc. and Radiat. Transfer **91**, No. 2, 233–244 (2005).
3. R.N. Halthore, D. Crisp, S. Schwartz, G.P. Anderson, A. Berk, B. Bonnel, O. Boucher, F.-L. Chang, M.-D. Chou, E. Clothiaux, P. Dubuisson, B. Fomin, Y. Fouquart, S. Freidenreich, C. Gautier, S. Kato, I. Laszlo, Z. Li, J.H. Mather, A. Plana-Fattor, V. Ramaswamy, P. Ricchiazzi, Y. Shiren, A. Trishchenko, and W. Wiscombe, J. Geophys. Res. **110**, D11206, doi:10.1029/2004JD005293 (2005).
4. R. Cahalan, R. Oreopoulos, A. Marshak, K.F. Evans, A. Davis, R. Pincus, K. Yetzer, B. Mayer, R. Davies, T. Ackerman, H. Barker, E. Clothiaux, R. Ellingson, M. Garay, E. Kassianov, S. Kinne, A. Macke, W. O'Hirok, P. Partain, S. Prigarin, A. Rublev, G. Stephens, E. Takara, T. Varnai, G. Wen, and T. Zhuravleva, Bull. of Amer. Meteorol. Soc. **86**, No. 9, 1275–1293 (2005).
5. V.E. Zuev and G.A. Titov, *Atmospheric Optics and Climate* (Publishing House "Spektr" of IAO SB RAS, Tomsk, 1996), 271 pp.
6. D. Lane-Veron and R. Somerville, J. Geophys. Res. **109**, D18113, doi: 10.1029/ 2004JD004524 (2004).
7. S.V. Afonin, V.V. Belov, and I.Yu. Makushkina, Atmos. Oceanic Opt. **7**, No. 6, 423–429 (1994).
8. V.E. Zuev, V.V. Belov, and V.V. Veretennikov, *System Theory in Optics of Disperse Media* (Publishing House "Spektr" of IAO SB RAS, 1997), 402 pp.
9. V.V. Belov and S.V. Afonin, *From Physical Fundamentals, Theory, and Simulation to Thematic Processing of Satellite Images* (Publishing House of IAO SB RAS, Tomsk, 2005), 266 pp.
10. G.M. Krekov, Atmos. Oceanic Opt. **20**, No. 9, 757–766 (2007).
11. G.I. Marchuk, G.A. Mikhailov, M.A. Nazaraliev, R.A. Darbinyan, B.A. Kargin, and B.S. Elepov, *Monte Carlo Method in Atmospheric Optics* (Nauka, Novosibirsk, 1976), 280 pp.
12. S.M. Ermakov and G.A. Mikhailov, *Statistical Simulation* (Nauka, Moscow, 1982), 296 pp.
13. B.A. Kargin, *Statistical Simulation of Solar Radiative Field in the Atmosphere* (Computer Center of SB of USSR Academy of Sciences, Novosibirsk, 1984), 206 pp.
14. A. Marshak and A. Davis, eds., *Radiative Transfer in Cloudy Atmosphere* (Springer-Verlag, 2005), 701 pp.
15. M.A. Nazaraliev, *Statistical Simulation of Radiative Processes in the Atmosphere* (Nauka, Novosibirsk, 1990), 227 pp.
16. *A Preliminary Cloudless Standard Atmosphere for Radiation Computation,* World Climate Research Programme. WCP-112, WMO/TD No. 24 (1986), 60 pp.
17. K.Ya. Kondratyev and D.V. Pozdnyakov, *Aerosol Models of the Atmosphere* (Nauka, Moscow, 1981), 103 pp.
18. V.E. Zuev and G.M. Krekov, *Optical Models of the Atmosphere* (Gidrometeoizdat, Leningrad, 1986), 256 pp.
19. G.A. d'Almeida, P. Koepke, and E. Shettle, *Atmospheric Aerosols: Global Climatology and Radiative Characteristics* (A Deepak Publishing, Hampton, Virginia, 1991), 420 pp.
20. M. Hess, P. Koepke, and I. Schult, Bull. Amer. Meteorol. Soc. **79**, No. 5, 831–844 (1998).
21. F.X. Kneizys, D.S. Robertson, L.W. Abreu, P. Acharya, G.P. Anderson, L.S. Rothman, J.H. Chetwynd, J.E.A. Selby, E.P. Shetle, W.O. Gallery, A. Berk, S.A. Clough, and L.S. Bernstein, *The MODTRAN 2/3 report and LOWTRAN 7 model* (Phillips Laboratory. Geophys. Directorate. Hanscom AFB, MA 01731–3010, 1996), 260 pp.
22. D. Deirmendjian, *Electromagnetic Scattering on Spherical Polydispersions* (Elsevier, 1969), 290 pp.
23. V.V. Sobolev, *Light Scattering in Atmospheres of Planets* (Nauka, Moscow, 1972), 335 pp.

24. S.M. Prigarin, *Foundations of Statistical Simulation of Optical Radiative Transfer. School Book* (Publishing House of Novosibirsk State University, Novosibirsk, 2001), 82 pp.
25. J. Lenoble, Radiative *Transfer in Scattering and Absorbing Atmospheres* (Gidrometeoizdat, Leningrad, 1990), 264 pp.
26. J.-J. Morcrette and Y. Fouquart, J. Atmos. Sci. **43**, No. 4, 321–328 (1986).
27. V.Ya. Galin, Atmos. Oceanic Opt. **12**, No. 3, 235–239 (1999).
28. K.A. Browning, Bull. Amer. Meteorol. Soc. **74**, No. 3, 387–399 (1993).
29. C.-H. Moeng, W. Cotton, C. Bretherton, A. Chlond, M. Khairoutdinov, S. Krueger, W. Lewellen, M. Mac-Vean, J. Pasquier, H. Rand, A. Siebesma, B. Stevens, and R. Sykes, Bull. Amer. Meteorol. Soc. **77**, No. 2, 261–278 (1996).
30. C. Bretherton, M. MacVean, P. Bechtold, A. Chlond, W. Cotton, J. Cuxart, H. Cuijpers, M. Khairoutdinov, B. Kosovic, D. Lewellen, C.-H. Moeng, P. Siebesma, B. Stevens, D. Stevens, I. Sykes, and M. Wyant, Quart. J. Roy. Meteorol. Soc. **125**, No. 554, 391–423 (1999).
31. A. Siebesma, C. Bretherton, A. Brown, A. Chlond, J. Cuxart, P. Duynkerke, H. Jiang, M. Khairoutdinov, D. Lewellen, C.-H. Moeng, E. Sanchez, B. Stevens, and D. Stevens, J. Atmos. Sci. **60**, No. 10, 1201–1219 (2003).
32. B. Stevens, C.-H. Moeng, A. Ackerman, C. Bretherton, A. Chlond, S. de Roode, J. Edwards, J.-C. Golaz, H. Jiang, M. Khairoutdinov, M. Kirkpatrick, D. Lewellen, A. Lock, F. Müller, D. Stevens, E. Whelan, and P. Zhu, Mon. Weather Rev. **133**, No. 6, 1443–1462, doi:10.1175/MWR2930.1 (2005).
33. K.F. Evans, J. Atmos. Sci. **55**, No. 3, 429–446 (1998).
34. O.V. Nikolaeva, L.P. Bass, T.A. Germogenova, A.A. Kokhanovsky, V.S. Kuznetsov, and B. Mayer, J. Quant. Spectrosc. and Radiat. Transfer **94**, Nos. 3–4, 405–424 (2005).
35. T.B. Zhuravleva, in: *Abstracts of the First and Second International Workshops on the Intercomparison of Three-dimensional Radiation Codes* (Tucson, Arizona, 2000), pp. 9–13.
36. T.B. Zhuravleva, in: *Abstracts of the First and Second International Workshops on the Intercomparison of Three-dimensional Radiation Codes* (Tucson, Arizona, 2000), pp. 104–105.
37. B. Mayer, in: *Abstracts of the First and Second International Workshops on the Intercomparison of Three-dimensional Radiation Codes* (Tucson, Arizona, 2000), pp. 49–54.
38. R. Cess, M. Zhang, G. Potter, V. Alekseev, H. Barker, S. Bony, R. Colman, D. Dazlich, A. Del Genio, M. Déqué, M. Dix, V. Dymnikov, M. Esch, L. Fowler, J. Fraser, V. Galin, W. Gates, J. Hack, W. Ingram, J. Kiehl, Y. Kim, H. Le Treut, X.-Z. Liang, B. McAvaney, V. Meleshko, J. Morcrette, D. Randall, E. Roeckner, M. Schelesinger, P. Sporyshev, K. Taylor, B. Timbal, E. Volodin, W. Wang, W.C. Wang, and R. Wetherald, J. Geophys. Res. D **102**, No. 14, 16593–16603 (1997).
39. E.M. Feigelson and L.D. Krasnokutskaya, Solar *Radiative Fluxes and Clouds* (Gidrometeoizdat, Leningrad, 1978), 157 pp.
40. B.M. Golubitskii and N.I. Moskalenko, Izv. Akad Nauk SSSR. Ser. Fiz. Atmos. Okeana **IV**, No. 3, 346–359 (1968).
41. N.I. Moskalenko, Izv. Akad. Nauk SSSR. Ser. Fiz. Atmos. Okeana **V**, No. 11, 1179–1190 (1969).
42. V.L. Filippov, Izv. Akad. Nauk SSSR. Ser. Fiz. Atmos. Okeana **IX**, No. 7, 774–775 (1973).
43. R. Goody, R. West, L. Chen, and D. Crisp, J. Quant. Spectrosc. and Radiat. Transfer **42**, No. 6, 539–550 (1989).
44. Q. Fu and K.N. Liou, J. Atmos. Sci. **49**, No. 22, 2139–2156 (1992).
45. K.M. Firsov, T.Yu. Chesnokova, V.V. Belov, A.B. Serebrennikov, and Yu.N. Ponomarev, Vychislit. Tekhnol. **7**, No. 5, 77–87 (2002).
46. T.B. Zhuravleva, I.M. Nasrtdinov, S.M. Sakerin, K.M. Firsov, and T.Yu. Chesnokova, Atmos. Oceanic Opt. **16**, No. 12, 972–981 (2003).
47. T.B. Zhuravleva and K.M. Firsov, Atmos. Oceanic Opt. **17**, No. 11, 799–806 (2004).
48. T.B. Zhuravleva and K.M. Firsov, Atmos. Oceanic Opt. **18**, No. 9, 696–702 (2005).
49. I.M. Nasrtdinov, T.B. Zhuravleva, and S.M. Sakerin, Atmos. Oceanic Opt. **19**, No. 10, 804–810 (2006).
50. W. O'Hirok and C. Gauttier, J. Atmos. Sci. **55**, No. 12, 2162–2179 (1998).
51. T.B. Zhuravleva, I.M. Nasrtdinov, and S.M. Sakerin, Atmos. Oceanic Opt. **16**, Nos. 5–6, 496–504 (2003).